Copper-Alumina Capsules for High-Temperature Thermal Energy Storage

Document Version
Accepted author manuscript

[Link to publication record in Manchester Research Explorer](#)

Citing this paper
Please note that where the full-text provided on Manchester Research Explorer is the Author Accepted Manuscript or Proof version this may differ from the final Published version. If citing, it is advised that you check and use the publisher's definitive version.

OPEN ACCESS

Copper-Alumina Capsules for High-Temperature Thermal Energy Storage

Bo Zhao[a], Renjie Liu[a], Nan Sheng[a], Yasser Mahmoudi[b], Chunyu Zhu[a]*

[a] School of Low-Carbon Energy and Power Engineering, China University of Mining and Technology, Xuzhou, 221116, China

[b] School of Engineering, The University of Manchester, Manchester, M13 9PL, UK

*Corresponding Author: zcyls@cumt.edu.cn

Abstract

High corrosivity, leakage and oxidation of metallic phase change materials (PCMs) have limited their applications in high-temperature thermal energy storage (TES) systems, regardless of their favorable benefits for high-temperature TES applications of over 1000 °C. To overcome these major challenges, this work presents a facial paraffin sacrificial layer approach for directly encapsulating copper (Cu) sphere PCM with alumina (Al_2O_3) shell, considering a buffer inner cavity. The cavity is formed by the decomposition of paraffin layer through a pre-sintered process. It plays a key role to accommodate the volume expansion of Cu core, thereby preventing the breakage of the shell and the leakage of the liquid PCM. A series of macrocapsules with different sizes (9.5 mm-21 mm) containing Cu core, cavity and Al_2O_3 shell are successfully produced using the paraffin sacrificial layer method and deploying two-step heat treatment. The experimental results show that the Al_2O_3 shell possesses a good structure, which can prevent the leakage of Cu core. The Al_2O_3 shell also has a strong compatibility with Cu core without any chemical reaction between two materials. At a temperature range of 1000-1100 °C, the calculated mass and volume energy storage densities of the PCM macrocapsule with 21 mm outer diameter are found to be 222 kJ/kg and 745 J/cm³, which are 1.83 and 1.76 times, respectively, higher than those for Al_2O_3 ceramic. After thermal cycle tests, the encapsulated Cu PCM shows a superior shape stability, chemical stability and thermal durability, which can be applied in long-term thermal storage system for high-temperature TES systems.

Keywords: Phase Change Material (PCM); Macro-encapsulation; High-temperature thermal energy storage; Thermal storage; Thermal management

1. Introduction

The global reality of the energy security crisis and rising gas and fossil fuel prices has demonstrated the importance of delivering future energy security through the greater use of renewable and clean sources of power, while seeking for efficient energy utilization.[1] Solar energy has received more attention and take a large proportion in energy sector because of the huge and widely distributed resources.[2, 3] Many technologies for solar energy harvest have rapidly developed globally, *e.g.*, photovoltaic power generation, solar hydrogen production and solar thermal utilization. Among various technologies of solar energy utilization, concentrated solar thermal power (CSP) is rapidly developing, which is integrated with the efficient thermal energy storage (TES) system.[4] Comparing to other solar energy harvest technologies, the CSP system can directly receive significant amount of thermal energy using reflector and solar power tower. The most attractive advantage of CSP plants is their integration with the TES system, which can store the excess solar energy during the daytime and release the thermal energy in nighttime, balancing the fluctuating power generation and maintaining a reliable power system.[5, 6] However, the efficiency of CSP stations needs to be further increased due to the exorbitant nominal levelized costs of electricity.

One main approach to increase the efficiency of a CSP system is to increase the operating temperature of the plant. In recent development of solar collection and solar concentration sections in a CSP, the thermal concentration technology has been developed rapidly resulting in temperatures of more than 1000 °C.[7] However, available materials and technology of TES systems are not functional to be operated in such high temperature operating conditions, hence preventing the further development of high efficiency CSP systems. Hence, the key to improve the efficiency of CSP stations is to develop innovative high-temperature materials for TES units.[8,9] High temperature leads to the greater work environment challenge and therefore require the enhanced properties of storage medium.[10] The key properties in high temperature work condition are: (1) enhancing mechanical strength of the TES medium (2) high degree of chemical stability between the medium and environment, (3) high energy density and thermal transfer ability of TES, and (4) enhanced thermal durability without thermal physical properties degradation during long-term application.[11]

The TES systems can be classified to sensible heat, latent heat and thermochemical heat storage systems. Presently, the CSP plants using molten salts as sensible heat storage media have been restricted to a maximum temperature of about 600 °C, which is unsuitable for next generation high-temperature CSP systems. Among these methods, latent heat thermal storage systems based on phase change materials (PCMs) have received more attention due to the high energy density as compared to sensible options and less system complexity when compared to thermochemical systems. Metallic PCMs have been recently regarded as suitable alternatives owing to their low-cost and high melting point.[12] Among these metallic materials, copper (Cu) is regarded as one of the most promising PCMs for high-temperature thermal storage because of its ultra-high melting point (>1000 °C), high thermal conductivity (398 W/m K) and high latent heat (208.7 kJ/kg).[13] However, if the molten liquid metal is directly used in a TES system, it may cause a crucial corrosion problem especially in high temperature operation system, resulting in the increase cost of corrosion protection equipment, the liquid leakage and the reduction of system lifetime.[14,15]

By encapsulating Cu sphere as-surrounded by a stable shell, the molten liquid Cu will not be in direct contact with the heat exchange media, resolving the leakage and corrosion problems, while increasing the heat transfer surface area, thereby increasing the heat transfer efficiency of the TES unit. Zhou et al.[16] successfully encapsulated the copper-based materials in Al_2O_3 based shell by an in situ sealing method, which were used for long-term air exposure cycling test with unfortunately observable degradation. Zhang et al.[17,18] prepared Ni-Cr or Fe shell on solid Cu balls by electroplating or pneumatic suspension method, respectively. However, the thermal energy storage density was decreased due to the high proportion of shell layer. Sheng et al.[19,20] successfully encapsulated the Cu powders and Cu-Ge powders by direct encapsulation method. This method is very effective for the encapsulation of powder core raw materials. However, in the control test, the macrocapsules based on solid Cu balls showed cracks and leakage after sintering process. For encapsulation, ceramics were found to be highly compatible and less prone to react with molten-metal in high temperature applications.[21] In comparison to microcapsules (with PCM spheres diameter of < 1 mm), the macrocapsules (with PCM spheres diameter of > 1 mm) present a higher ratio of core to shell, resulting in a higher thermal energy density of the TES systems.[22] However, due to the large volume expansion of Cu-based PCMs at high temperatures, the shells of the capsules may crack during the phase change transition, resulting in the leakage of the liquid metals.[23-25] To overcome this issue, the sacrificial layer method can

smartly create a buffer cavity inside the macrocapsules. Mathur et al. [26] coated the sacrificial layer and shell on the core for inorganic salt mixture PCM by fluid bed method. Alam, T. E et al.[27] pressed the polymer particles on the core in a hydraulic press at 980 N of force to form a thin polymeric film sacrificial layer. These methods need the equipment such as fluid bed or hydraulic press to form the sacrificial layer in the preparation process. In an earlier study, the authors have deployed a sacrificial layer method for encapsulation of Al PCM by an alumina shell and tested the capsules up to temperature of ~700 °C. [28] Although the results highlighted the advantageous of the sacrificial layer method for encapsulation, the Al capsules were not durable for higher temperatures required for application for next generation concentrated solar power stations. In the present study, the simple paraffin sacrificial layer method was used to encapsulate Cu metal with alumina shell for high temperatures >1000 °C. The cavity is formed by paraffin layer which is decomposed during the calcination process, ensuring the successfully encapsulation of Cu spheres under high temperature. These capsules can be used for high temperature TES system for next generation CSP station, especially based on supercritical CO_2 Brayton cycle.[29]

2. Experiment

2.1. Materials

Copper (Cu) (Guangdong Jinming hardware Machinery, 99.9%) spheres with diameters of 5 mm, 8 mm, 15 mm were used as the core PCM. Carboxymethyl cellulose (CMC) (Macklin, M.W.

250000(DS=0.9), 1500-3100mPa.s) was used as binder and Al_2O_3 (Macklin, 99.99%, 5 ~ 6 μm)

were used as shell material. Paraffin (Shanghai Joule Wax Co. LTD, oil content 1.5 %) with melting point of 52.5 °C-55 °C was used as the sacrificial layer materials.

2.2. Fabrication of encapsulated PCM

A capsule is consisted of a Cu sphere core, a cavity created by paraffin and a shell made of Al_2O_3 (named as Cu@cavity@Al_2O_3 in this paper). The preparation process of Cu@cavity@Al_2O_3 macrocapsule is shown in Fig. 1. The core of the macrocapsules are made of Cu spheres with different diameters (5 mm, 8 mm and 15 mm) without any treatment. The solid paraffin was melted into liquid in water bath pot under 70 °C, ensuring that it can be easily adhered on the Cu spheres. Then the Cu spheres were taken out from the liquid paraffin and rolled on an Al foil, thereby the excess paraffin was adhered on the Al foil and the remaining paraffin was solidified at room temperature. The 5mm Cu balls were immersed in paraffin wax once, while the 8 mm and 15mm diameter Cu balls were immersed in paraffin wax two times. The Cu spheres coated by paraffin sacrificial layer with desired thickness were obtained, named as Cu@paraffin.
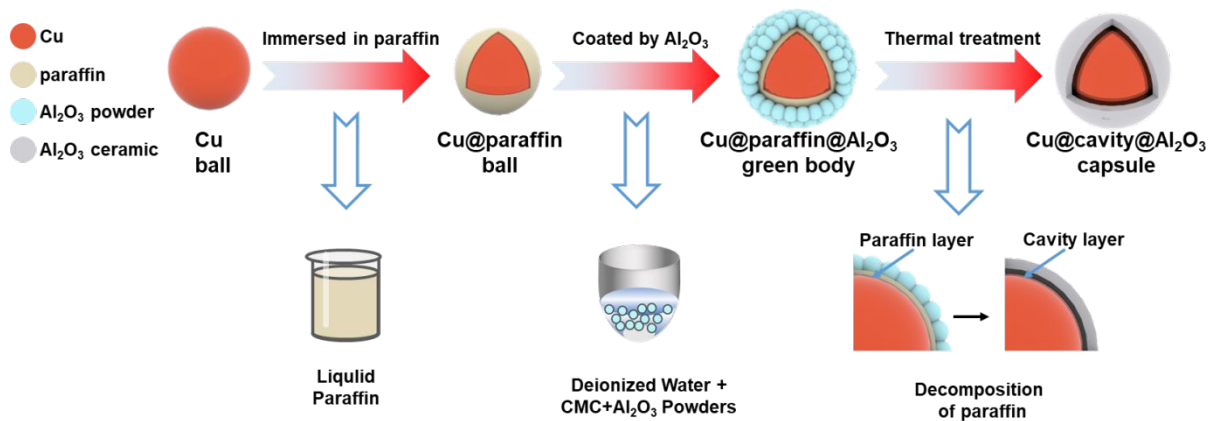
Figure 1. The schematic diagram of preparation process of Cu@cavity@Al$_2$O$_3$ macrocapsule.

Subsequently, the carboxymethyl cellulose (CMC) was dissolved into deionized water for obtaining a gel mixture. After adding the Al$_2$O$_3$ powders into the gel mixture, the viscous shell materials were obtained. The green body macrocapsules were prepared by coating the shell materials on the Cu@paraffin spheres, named as Cu@paraffin@Al$_2$O$_3$. After drying, the green-bodies were pre-sintered in a muffle furnace at 420 °C for 2 hours and then sintered in a tube furnace under argon (Ar) atmosphere at 1200 °C for 2 hours. The sacrificial layer cavity was obtained after pre-sintering process and the final macrocapsules were prepared after sintering process, named as Cu@cavity@Al$_2$O$_3$. The Cu spheres were also directly coated with the Al$_2$O$_3$ shell mixture without the introduction of paraffin layer, to prepare the comparing samples of Cu@Al$_2$O$_3$.

2.3. Characterization
The macro-morphology of the macrocapsules at different stages were observed by digital camera. The micromorphology and microstructure of samples were evaluated using high-resolution field emission scanning electron microscope (SEM) (MA1A3 FSEM, Tescan, Czech Republic). The crystallite phase compositions of samples were analyzed using X-ray diffraction method (XRD) (D8ADVANCE, Bruker, German). The thermal properties including melting temperature, solidification temperature and phase change enthalpy of Cu PCM were measured in an argon atmosphere with a 5 °C/min heating and solidification rate using a differential scanning calorimeter (DSC) (STA449 F5, Nezsch, German). In the DSC test, we selected three cores with different diameters to test. Each sample was tested twice and the data of the second time was taken as the experimental result. The test sample was about 10 mg and the error of three measurements was ± 1 J/g. To evaluate the thermal durability and shape stability of Cu@cavity@Al$_2$O$_3$ capsules, heating-cooling cycle tests were performed between 1000 °C to 1200 °C under Ar atmosphere with a rate of 2 °C/min in a tube furnace. The morphology, weight and thermal properties of macrocapsules were observed after certain cycles, in order to evaluate the stability of properties. After thermal cycles, the three cores with different diameter were also tested by DSC.

3. Results and Discussion
3. 1. Structure and Morphology of the Macrocapsules

The morphology of macrocapsule including the control group and test group were analyzed by optical photograph for observing the breakage of Al$_2$O$_3$ shell. Fig. 2 shows the morphology of

control group macrocapsules in different preparation stages. According to the diameters of the Cu core balls (d_c) and thickness of Al_2O_3 shell (d_s), the macrocapsules were named as $d_c@d_s$, including 5mm@2mm, 8mm@2.5mm, 15mm@2.5mm. The Cu spheres were solid spheres with smooth surface, and after being coated by Al_2O_3 shell, the obtained dried capsules still maintained a good degree of sphericity without any breakage on the Al_2O_3 shell (see Fig. 2). However, all the group of macrocapsule either broken or showed cracks on the shells after being pre-sintered at 420 °C and a black layer appears on the Cu sphere core. The mixture of Al_2O_3 and CMC was used as shell materials for this study because the Al_2O_3 presented a good chemical stability and strength, and the CMC could bond the Al_2O_3 powders together at the room temperature. Hence, the macrocapsule showed a good model without cracks at the room temperature. However, the Cu spheres had a thermal volume expansion with the temperature increase, causing a high thermal stress on the shell. The black layer materials could be caused by the Cu core partial oxidation in the pre-sintering process under air atmosphere.
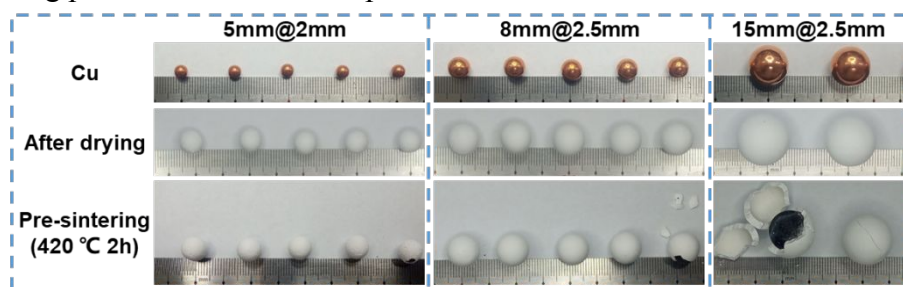

Figure 2. The optical images of the control group samples prepared by the direct coating method for different diameters and thicknesses of 5mm@2mm, 8mm@2.5mm and 15mm@2.5mm as obtained at different preparation stages (solid Cu balls, dried capsules and pre-sintered capsules).

In the above discussion of control group, the directly encapsulation method did not overcome the thermal stress problem caused by the Cu metal volume expansion and the volume shrinkage of shell at high temperature, resulting in cracks and failure of the shells. To address this critical problem, in the thermal treatment process, a cavity layer into the macrocapsule was further introduced by the decomposition of paraffin as a sacrificial layer. This offers a buffer space that can accommodate the huge thermal volume expansion of Cu and volume shrinkage of Al_2O_3 shell during the heating process. Additionally, the thickness of paraffin layer was determined by the coating times, resulting in a controllable cavity in macrocapsules. First, the Cu spheres and the Al_2O_3 mixture were used as the core and shell materials of macrocapsules, respectively, which were consistent with the control group. Then the layer of paraffin was coated on the Cu sphere before encapsulating the Cu spheres by Al_2O_3 shell. The volume expansion of Cu core was increased with the diameter of Cu spheres. Hence, the samples with different thickness of cavity were produced, ensuring the macrocapsules with suitable buffer space. Fig. 3 shows the optical photographs of Cu@cavity@Al_2O_3 macrocapsules at different stages of preparation. The obtained final macrocapsules were named as 5mm@0.25mm@2mm, 8mm@0.5mm@2.5mm, 15mm@0.5mm@2.5mm, according to the diameter of Cu core, the thickness of paraffin layer and the thickness of Al_2O_3 shell, respectively.

It can be seen in Fig. 3 that the paraffin layer was uniformly coated on the Cu sphere, forming the Cu@paraffin with a good spherical degree. By cutting a macrocapsule, the Cu core, cavity and the cross section of Al_2O_3 shell could be clearly observed from Fig. 4. Comparing with the control group, the pre-sintered samples in this group have not broken nor have cracks on the shells. After

being sintered under 1200 ℃, the Cu core underwent a process of melting into liquid copper and solidification into solid copper, appearing the red color and a smooth surface. The black film has disappeared because of the copper oxide has reacted with the remaining carbon under Ar atmosphere, resulting the copper oxide has been reduced to copper. There are no holes and cracks on the Al_2O_3 shells. Hence, it is confirmed that the Cu core could be encapsulated efficiently with Al_2O_3 shell by using the paraffin sacrificial layer method.
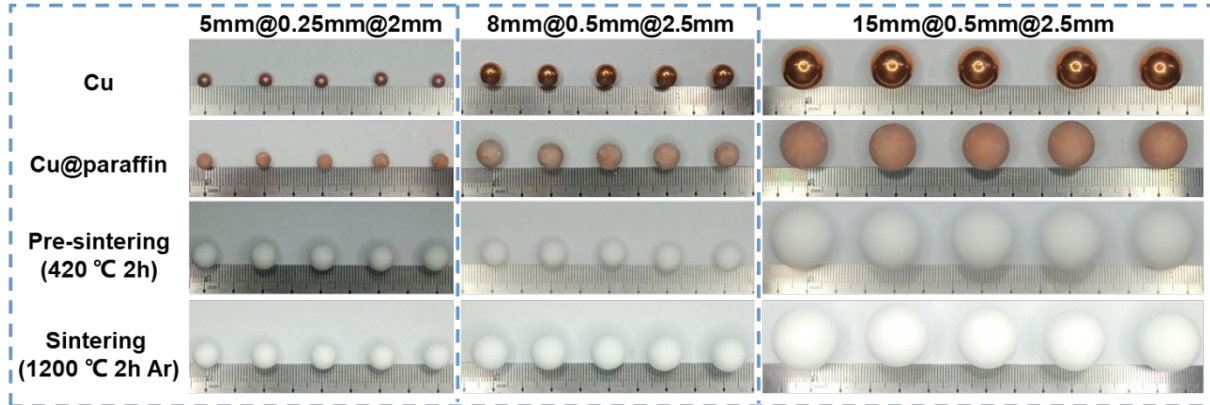

Figure 3. The optical pictures of macrocapsules prepared by sacrificial layer method (5 mm@0.25 mm@2 mm, 8 mm@0.5 mm@2.5 mm, 15 mm@0.5 mm@2.5 mm) obtained at different preparation stages (solid Cu balls, Cu@paraffin capsules, pre-sintered capsules, and sintered capsules).
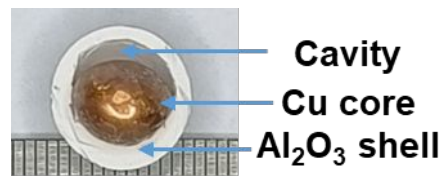

Figure 4. The opened 8mm@0.5mm@2.5mm capsule after sintering process.

Compatibility of the encapsulating materials with molten metal-based PCMs is crucial for the present application. We cut one macrocapsule with 14 mm diameter for XRD and SEM testing. Fig. 5 shows the XRD patterns of core and shell materials before and after being calcined at 1200 ℃. In the XRD pattern, it is found that the main diffractive peak of core material located at 2θ=43.3° and 50.4° which corresponded to the (1 1 1) and (2 0 0) planes of the Cu phase (PDF#04-0836). It is also observed that the diffractive peak intensities of shell material at the positions of 2θ=25.6°, 35.1°, 37.8°, 43.4°, 52.5°, 57.5°, 66.5° and 68.2° due to the (012), (104), (110), (024), (116), (214) and (300) planes of α-Al_2O_3 (PDF#10-0173). After the Cu sphere core being melted into liquid and then being solidified under high temperature, the XRD pattern of core and shell materials are still consistent with the standard PDF card. It infers that the Al_2O_3 ceramic is a suitable shell material for the metal encapsulation, which can overcome the high corrosiveness of metal based PCMs under high temperature.
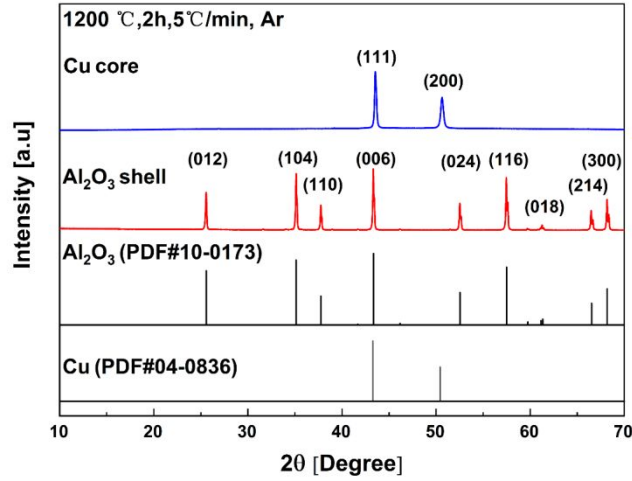
Figure 5. XRD patterns of capsules after sintering at 1200 ℃.

The cross section of the Al_2O_3 shell was analyzed by SEM for measuring the microstructure details of the sintered ceramics. From SEM images in Fig. 6, the shell presented homogenously sintered Al_2O_3 powders, forming a well-constructed shell without cracks. As can be seen from Fig. 6 (b) and (c), some pores between particles are visible which might be attributed to the decomposition of CMC binder and the relatively low sintering temperature, thereby the shell was still not completely condensed. However, the as-sintered shell is enough stable to encapsulate the inner metal liquid.
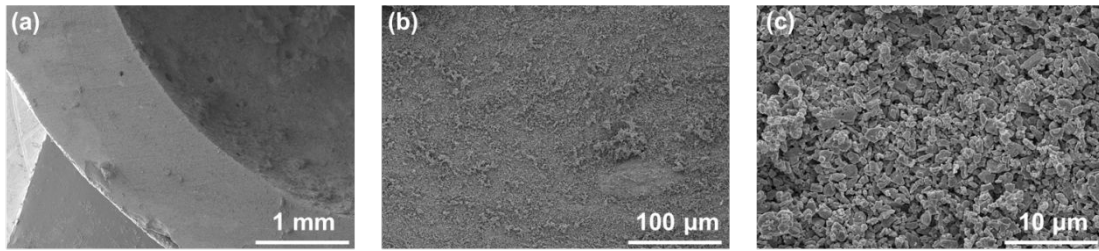

Figure 6. SEM images of Al_2O_3 shell after sintering at 1200 ℃.

3.2. Thermal Storage Performance

The macrocapsule is composed of Cu PCM as the core and Al_2O_3 ceramic shell, representing as latent heat and sensible heat storage materials, respectively. Hence, the thermal storage capability of macrocapsule was composed of phase change enthalpy of Cu core and sensible heat of Cu core and Al_2O_3 shell. The thermal storage value can be calculated by the following equation:

$$Q = m_{core}\Delta h_m + \int_{T_1}^{T_2} C_{shell} m_{shell} + \int_{T_1}^{T_2} C_{core} m_{core} \tag{2}$$

where, Q is the total effective thermal energy stored in the macrocapsule. The latent heat enthalpy of Cu was measured using the DSC. In the equation, the first term is the latent heat storage of Cu core, the second term is the sensible heat storage of Al_2O_3 shell, and the last term is the sensible heat storage of Cu core. m_{core} and m_{shell} are the mass of Cu core and Al_2O_3 shell, respectively. Here, the sensible heat was associated with the working temperature range, where T_1 and T_2 is the start temperature and end temperature respectively. C_{core} and C_{shell}, representing the specific heat capacity of Cu core and Al_2O_3 shell respectively, are a function of temperature, which are exported from a thermodynamic database of HSC Chemistry 9.0 software. In this study, we chose

three temperature ranges, i.e., 900-1100 °C, 1000-1100 °C and 1000-1200 °C, according to the melting temperature of Cu core and work temperature. To evaluate the thermal storage performance of macrocapsules and the comparable ceramic balls, the mass heat storage density ($q_m = Q/m$) and volumetric heat storage density ($q_v = Q/v$) were calculated, where m and v represent the mass and volume of the samples, respectively.

It is seen in Fig. 7 that the latent heat storage of Cu core measured by DSC instrument yields a high phase transition temperature and suitable phase change enthalpy. There is only one endothermic peak occurred at around 1063 °C, indicating the solid-liquid phase transition process. In the cooling process, the exothermic peak appears at around 1044 °C showing the shift toward lower temperature than the melting point, which is due to the supercooling characteristics. Compared to the standard sample, the melting enthalpy and freezing enthalpy are the same as 214 J/g. The good thermal physical properties endow the Cu core could work in high temperature application.
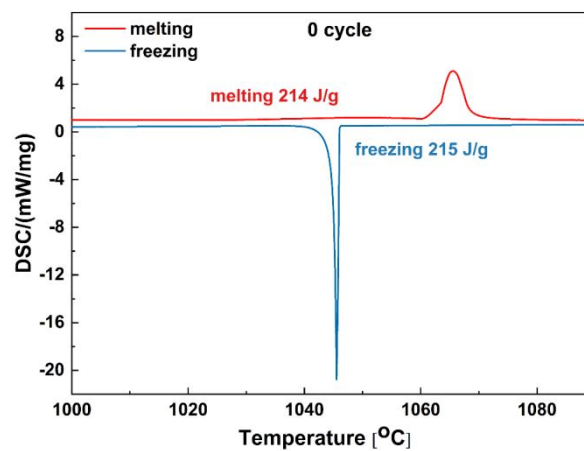

Figure 7. DSC test of pure Cu ball before thermal cycles.

Fig. 8(a) and (b) show the results of mass thermal storage density and volume thermal storage density, respectively. In Fig. 8, the x-axis represents the calculated temperature range, and the y-axis represents the heat storage density. The black marks on the bar chart represent the heat storage density of the samples. The ratios marked with red color on the bar chart represent the ratios of thermal storage in the core to that in the shell. The calculated samples include 5mm@0.25mm@2mm, 8mm@0.5mm@2.5mm, 15mm@0.5mm@2.5mm and Al_2O_3 ceramic.
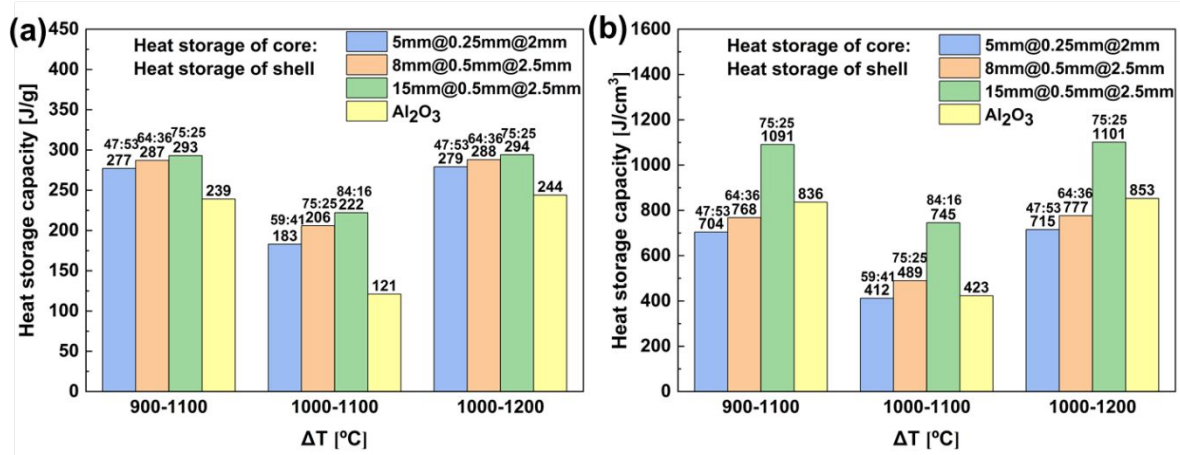
Figure 8. Thermal energy density of macrocapsules at different temperature ranges, (a) mass thermal storage density and (b) volume thermal storage density

It is seen in Fig. 8 that the mass thermal storage density of all different size macrocapsules were higher than pure ceramics due to the larger phase change thermal storage of Cu core. However, only the large capsule sample 15mm@0.5mm@2.5mm shows a superior volume thermal energy density compared to Al_2O_3 ceramics. This is mainly because of that the cavity does not contribute to the thermal storage capability of the capsule. Hence, under the same size, the smaller cavity ratio could enhance the volume thermal storage density of the macrocapsule. It should also be noted that the thermal energy density is increased with the size of macrocapsule increase, which is mainly due to the higher mass ratio of core to shell. It is seen Table 1 that the macrocapsule possess a higher ratio of core to shell when the size of macrocapsule is increased and the highest ratio is 71:29, resulting a larger proportion of thermal energy storage for Cu core. The highest mass and volume energy storage densities of macrocapsule reached 294 J/g and 1101 J/cm³ in a temperature range of 1000 °C -1200 °C, which are 1.2 and 1.3 times higher than Al_2O_3 pure ceramics, respectively. At a temperature range of 1000-1100 °C, the energy density of 15mm@0.5mm@2.5mm capsule reach 222 kJ/kg and 745 J/cm³, which are 1.83 and 1.76 times respectively higher than those for Al_2O_3 ceramic. This indicates that the macrocapsules have a superior thermal energy storage density than ceramic sensible balls for high temperature application.

Table 1. Mass of Cu core and Al_2O_3 shells for macrocpasurles with different diameters.

Sample	m_{core} (g)	m_{shell} (g)	m_{core}:m_{shell}
5mm@0.25mm@2mm	0.585	0.817	42:58
8mm@0.5mm@2.5mm	2.327	1.593	59:41
15mm@0.5mm@2.5mm	15.740	6.432	71:29

3.3. Cycle durability test

The durability of the fabricated macrocapsules was evaluated by heating-cooling cyclic tests performed by repeating melting and solidification processes. The macrocapsules were cycled between 1000 °C and 1200 °C, dwelling at initial and final temperatures for 30 min. Fig. 8 shows the thermal cycling profile of macrocapsule which have successfully passed after 150 thermal cycles. As shown in Fig. 10, By cutting a sample, the Cu core and the Al_2O_3 shell are clearly observed.
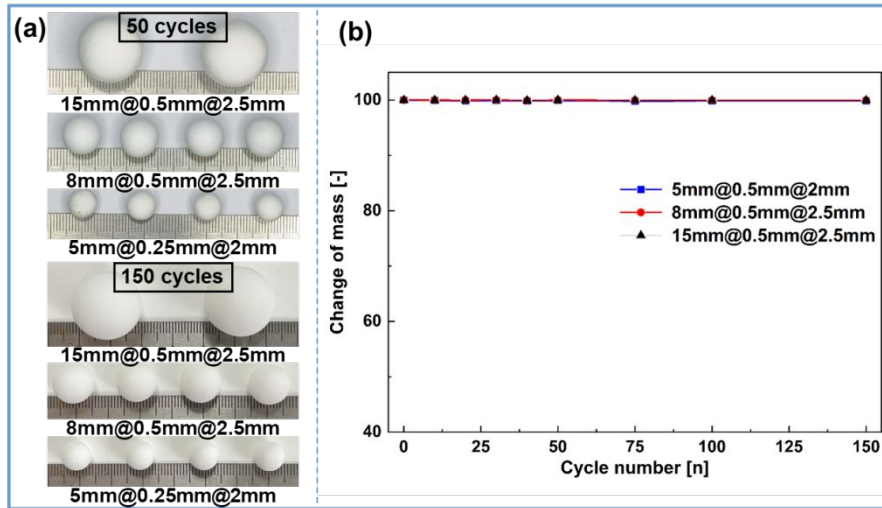
Figure 9. Heating-cooling cyclic tests, (a) the optical images of 50th and 150th cycle numbers, and (b) change in the macrocapsule mass with respect to the initial mass for different cycle numbers.
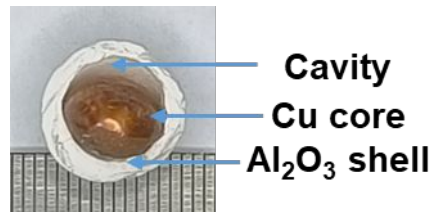

Figure 10. The opened 8mm@0.5mm@2.5mm capsule after 150 thermal cycles.

The optical images of cycled macrocapsules after 50 and 150 cycles were shown in Fig. 9(a). It is seen that for macrocapsules as-tested, there are no cracks or failure of the samples after 150 cycles. The shedding of shell materials also did not occur on the surface of macrocapsules, maintaining a good shape stability. The mass of macrocapsules was recorded after thermal cycles and the ratio of mass change with respect to the initial mass was shown in Fig. 9(b). It is seen that the mass of all capsules remained unchanged during the thermal cycled melting and solidification process. This further confirms that the cavity inside the capsule accommodate the volume expansion/shrinkage of Cu during the high temperature melting and solidification cycles, indicating that the paraffin sacrificial layer method was suitable for the encapsulation of Cu core. In the inert gas atmosphere, the macrocapsules present a suitable stability performance.

After thermal cycling, we cut one macrocapsule with 14 mm diameter, and the core and shell materials were also evaluated by XRD test. The results were shown in Fig. 11. It is seen in Fig. 11(d) that the peak intensities and position of Cu core and Al_2O_3 shell have no changes, which are also consistent with the XRD patterns of standard PDF cards. Therefore, it can be inferred that the spheres of molten Cu have no impact on ceramic Al_2O_3 shell under high temperature thermal cycles. These results suggest that the Cu core and Al_2O_3 shell are chemically compatible at high temperature thermal cycles without any chemical reactions, showing a good chemical stability of macrocapsules. To further characterize the detailed structure of Al_2O_3 shell after 150 thermal cycles, the sample were analyzed using the SEM technique and the results are shown in Figs. 11a-11c. In comparison to the base samples (before thermal cycling), the cross section of Al_2O_3 shell does not change significantly. The pores of Al_2O_3 shell were not filled by liquid Cu, which is still visible after 150 cycles. These observations indicate that the macrocapsule possess a good chemical stability during thermal cycles.
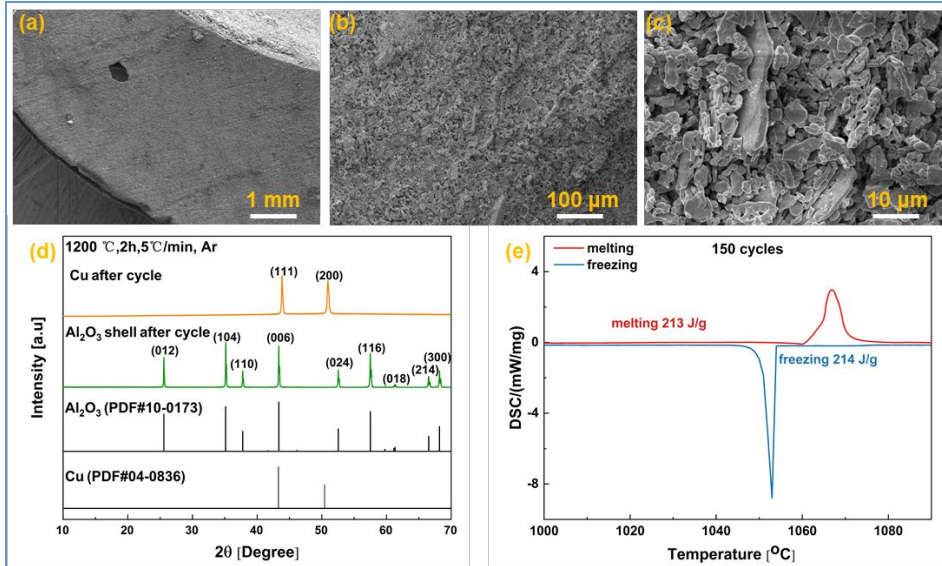
10

Figure 11. The test of macrocapsule after 150 thermal cycles, (a-c) SEM images of Al_2O_3 shell, (d) XRD results of the core and the shell, and (e) DSC test of Cu core PCM.

The phase change enthalpy of Cu core after 150 thermal cycles was evaluated by the DSC test. Fig. 11(e) shows that the enthalpies of melting and freezing process are 213 J/g and 214 J/g, respectively, similar to the values for base samples (before thermal cycling). At various stages of thermal cycling, the DSC curves of Cu core shows no significant change in their thermophysical properties, demonstrating a good thermal cycle stability of the encapsulated PCM. In conclusion, the results of various tests as-conducted confirm that the macrocapsule containing Cu core, cavity and Al_2O_3 shell possess a good shape stability, chemical stability and thermal durability which can be applied in high-temperature thermal storage systems.

4. Conclusions

In this work a facial technique based on paraffin sacrificial layer method was deployed to produce encapsulated metallic PCMs suitable for high temperature (>1000 °C) thermal energy storage applications. The core of the capsule was made of Cu and a shell made of Al_2O_3 with a cavity between the core and the shell, named Cu@cavity@Al_2O_3. The Al_2O_3 shell prevents metal corrosion due to its compatibility with molten metal material. The cavity was the key for the successful direct encapsulation of commercial Cu sphere which could accommodate the volumetric expansion of the Cu core during the heating and melting process. The size of cavity could be controlled by controlling the thickness of paraffin layer. Macrocapsule samples with diameter in the range of [9.5 mm-21 mm] were fabricated and tested under heating-cooling cycles between 1000 °C to 1200 °C. After being sintered, the macrocapsules without cavity were broken due to the volume expansion of the Cu sphere during the heating process. While the macrocapsules with cavity remain intact during the sintering process and have survived more than 150 thermal cycles during the cyclic test, showing a good shape stability, good chemical stability and no degradation in their thermo-physical properties, thereby making them suitable for high-temperature long-term storage. The macrocapsule with cavity and outer diameter of 21 mm yields a high melting temperature and thermal energy storage density, reaching 222 kJ/kg and 745 J/cm³ at 1000-1100 °C temperature region, which are 1.83 and 1.76 times respectively higher than those for Al_2O_3 ceramic balls. The energy density of macrocapsules was increased with the capsule diameter, because of the increased ratio of core to shell. Hence, the development of capsules with

high core-shell ratio could further increase the thermal energy density. Based on these results, it can be concluded that the developed ceramics coated capsules of high temperature metallic PCMs can be used in high temperature latent heat storage systems central receiver solar power plants.

Declaration of Competing Interest

The authors declared that they have no conflicts of interest to this work. We declare that we do not have any commercial or associative interest that represents a conflict of interest in connection with the work submitted.

References

(1) Sinsel, S. R.; Riemke, R. L.; Hoffmann, V. H., Challenges and solution technologies for the integration of variable renewable energy sources—a review. *Renewable Energy* **2020,** *145*, 2271-2285.

(2) Ding, W.; Bauer, T., Progress in Research and Development of Molten Chloride Salt Technology for Next Generation Concentrated Solar Power Plants. *Engineering* **2021,** *7* (3), 334-347.

(3) He, Y.-L.; Qiu, Y.; Wang, K.; Yuan, F.; Wang, W.-Q.; Li, M.-J.; Guo, J.-Q., Perspective of concentrating solar power. *Energy* **2020,** *198,* 117373.

(4) Palacios, A.; Barreneche, C.; Navarro, M. E.; Ding, Y., Thermal energy storage technologies for concentrated solar power – A review from a materials perspective. *Renewable Energy* **2020,** *156*, 1244-1265.

(5) Pereira da Cunha, J.; Eames, P., Thermal energy storage for low and medium temperature applications using phase change materials – A review. *Applied Energy* **2016,** *177*, 227-238.

(6) Opolot, M.; Zhao, C.; Liu, M.; Mancin, S.; Bruno, F.; Hooman, K., A review of high temperature (≥ 500 °C) latent heat thermal energy storage. *Renewable and Sustainable Energy Reviews* **2022,** *160,* 112293.

(7) Caron, S.; Garrido, J.; Ballestrín, J.; Sutter, F.; Röger, M.; Manzano-Agugliaro, F., A comparative analysis of opto-thermal figures of merit for high temperature solar thermal absorber coatings. *Renewable and Sustainable Energy Reviews* **2022,** *154,* 111818.

(8) Muto, A.; McCabe, K.; Real, D., High-temperature calcium-based thermochemical energy storage system for use with CSP facilities. 2018.

(9) Padilla, R. V.; Soo Too, Y. C.; Benito, R.; Stein, W., Exergetic analysis of supercritical CO_2 Brayton cycles integrated with solar central receivers. *Applied Energy* **2015,** *148*, 348-365.

(10) Liu, M.; Omaraa, E. S.; Qi, J.; Haseli, P.; Ibrahim, J.; Sergeev, D.; Müller, M.; Bruno, F.; Majewski, P., Review and characterisation of high-temperature phase change material candidates between 500 C and 700°C. *Renewable and Sustainable Energy Reviews* **2021,** *150,* 111528.

(11) Xu, B.; Li, P.; Chan, C., Application of phase change materials for thermal energy storage in concentrated solar thermal power plants: A review to recent developments. *Applied Energy* **2015,** *160,* 286-307.

(12) Koide, H.; Kurniawan, A.; Takahashi, T.; Kawaguchi, T.; Sakai, H.; Sato, Y.; Chiu, J. N. W.; Nomura, T., Performance analysis of packed bed latent heat storage system for high-

temperature thermal energy storage using pellets composed of micro-encapsulated phase change material. *Energy* **2022,** *238,* 121746.

(13) Gokon, N.; Jie, C. S.; Nakano, Y.; Okazaki, S.; Kodama, T.; Hatamachi, T.; Bellan, S., Phase Change Material of Copper–Germanium Alloy as Solar Latent Heat Storage at High Temperatures. *Frontiers in Energy Research* **2021,** *9,* 696213.

(14) Zhang, S.; Li, Z.; Yao, Y.; Tian, L.; Yan, Y., Heat transfer characteristics and compatibility of molten salt/ceramic porous composite phase change material. *Nano Energy* **2022,** *100,* 107476.

(15) Sarvghad, M.; Delkasar Maher, S.; Collard, D.; Tassan, M.; Will, G.; Steinberg, T. A., Materials compatibility for the next generation of Concentrated Solar Power plants. *Energy Storage Materials* **2018,** *14,* 179-198.

(16) Zhou, X.; Yamashita, S.; Kubota, M.; Kita, H., Encapsulated Copper-Based Phase-Change Materials for High-Temperature Heat Storage. *Acs Omega* **2022,** *7* (6).

(17) Ma, B.; Li, J.; Xu, Z.; Peng, Z., Fe-shell/Cu-core encapsulated metallic phase change materials prepared by aerodynamic levitation method. *Applied Energy* **2014,** *132,* 568-574.

(18) Zhang, G.; Li, J.; Chen, Y.; Xiang, H.; Ma, B.; Xu, Z.; Ma, X., Encapsulation of copper-based phase change materials for high temperature thermal energy storage. *Solar Energy Materials and Solar Cells* **2014,** *128,* 131-137.

(19) Sheng, N.; Ge, Y.; Guo, Y.; Zhu, C.; Rao, Z., Macro-encapsulated metallic phase change material over 1000 °C for high-temperature thermal storage. *Solar Energy Materials and Solar Cells* **2022,** *239,* 111655.

(20) Ge, Y.; Guo, Y.; Sheng, N.; Zhu, C., Fabrication of Cu–Ge macrocapsules using ceramic shells by powder formation method for high-temperature thermal energy storage. *Solar Energy Materials and Solar Cells* **2023,** *253,* 112224.

(21) Jacob, R.; Bruno, F., Review on shell materials used in the encapsulation of phase change materials for high temperature thermal energy storage. *Renewable and Sustainable Energy Reviews* **2015,** *48,* 79-87.

(22) Yu, D.-H.; He, Z.-Z., Shape-remodeled macrocapsule of phase change materials for thermal energy storage and thermal management. *Applied Energy* **2019,** *247,* 503-516.

(23) Sun, Z.; Zou, L. Y.; Cheng, X. M.; Zhu, J. Q.; Li, Y. Y.; Zhou, W. B., Fabrication, Structure, and Thermal Properties of Mg-Cu Alloys as High Temperature PCM for Thermal Energy Storage. *Materials* **2021,** *14* (15).

(24) Sun, Z.; Li, L. F.; Cheng, X. M.; Zhu, J. Q.; Li, Y. Y.; Zhou, W. B., Thermal Properties and the Prospects of Thermal Energy Storage of Mg-25%Cu-15%Zn Eutectic Alloy as Phase Change Material. *Materials* **2021,** *14* (12).

(25) Villada, C.; Rawson, A.; Navarrete, N.; Kolbe, M.; Kargl, F., Copper-magnesium eutectic as phase change material for thermal storage applications: Thermophysical properties and compatibility. *Journal of Energy Storage* **2022,** *52,* 105069.
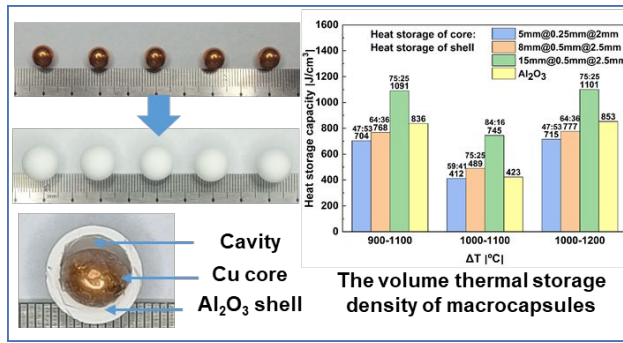
(26) Mathur, A.; Kasetty, R.; Oxley, J.; Mendez, J.; Nithyanandam, K. In Using encapsulated phase change salts for concentrated solar power plant, International Conference of the SolarPACES **2013,** *48,* 908-915.

(27) Alam, T. E.; Dhau, J. S.; Goswami, D. Y.; Stefanakos, E., Macroencapsulation and characterization of phase change materials for latent heat thermal energy storage systems. *Applied Energy* **2015,** *154,* 92-101.

(28) Zhao, B.; Guo, Y.; Wang, C.; Zeng, L.; Gao, K.; Sheng, N.; Gariboldi, E.; Zhu, C., Development of over 3000 cycles durable macro-encapsulated aluminum with cavity by a sacrificial

layer method for high temperature latent heat storage. *Chemical Engineering Journal* **2023,** *457,* 141352.

(29) Yang, J.;   Yang, Z.; Duan, Y., Load matching and techno-economic analysis of CSP plant with S–CO$_2$ Brayton cycle in CSP-PV-wind hybrid system. *Energy* **2021,** *223,* 120016.

The TOC graphic.